Ground Support 2026 - D Cumming-Potvin & J Wesseloo (eds.)
© 2026 Australian Centre for Geomechanics, Perth
doi:10.36487/ACG_repo/2625_06

Indoor laboratory dynamic repeated drop testing of shotcrete–mesh–rockbolt ground support system

Xin Wang [a,b,*], Jialong Guo [a], Zhiyuan Zhang [a]

[a] *State Key Laboratory of Intelligent Deep Metal Mining and Equipment, Northeastern University, China*

[b] *China National Gold Group Co., Ltd., China*

Abstract

Surface support systems in burst-prone underground excavations are required to retain fractured rock and accommodate repeated dynamic loading. However, the influence of mesh specification and shotcrete cracking on the system response is still not well quantified. This work presents an indoor full-scale impact testing program on ground support of a shotcrete–mesh–rockbolt panel. A newly developed test apparatus called FORTRESS-Dyna (Full-scale Observation, Research, Testing on Resistance Evaluation for Support System-Dynamic) is used to conduct the dynamic drop impact test. A C35 shotcrete panel reinforced with 8 mm welded mesh at 200 × 200 mm mesh spacing and eight 3.0 m rockbolts was subjected to 24 repeated drop impacts, with the drop height increasing from 20 to 60 cm. In the shotcrete–mesh–rockbolt test, it is found that cracking of the shotcrete led to progressive stiffness loss and rapid accumulation of residual displacement at high cumulative energy. The final cumulative nominal input energy reached 64.4 kJ by the end of the test. Even after cracking, the remaining rockbolts, plates and mesh continued to provide limited restraint before final instability. The whole test is divided into 4 distinct stages: relatively high stiffness phase, cracking-leading-softening phase, connection linking dominant failure phase, and large deformation and failure phase. The test results highlight the need to assess dynamic surface support using deformation, residual displacement, and connection behaviour, rather than the peak load alone.

Keywords: *dynamic ground support testing, welded mesh, shotcrete, residual displacement, surface support*

1 Introduction

Underground excavations in highly stressed ground usually are subjected to dynamic disturbances associated with mining-induced seismicity, blasting and local rock ejection. Under these conditions, ground support systems must not only reinforce the surrounding rock mass but also retain fractured rock and accommodate rapid deformation. Accordingly, support performance in burst-prone ground is commonly evaluated in terms of deformation capacity, energy dissipation and compatibility among support components, rather than load capacity alone (Cai 2024; Cai & Kaiser 2018; He et al. 2025; Kaiser & Moss 2022; Li 2021).

A ground support system normally consists of reinforcement elements and surface support. Rockbolts and cable bolts provide reinforcement within the rock mass, while mesh, plates, straps and shotcrete help retain fractured rock and transfer load to the reinforcement system. The dynamic behaviour of individual reinforcement elements has been widely investigated through pull tests, impact tests, momentum-transfer tests and energy-absorbing bolt development (Chunlin Li 2010; Knox 2023; Shou et al. 2024; Villaescusa & Potvin 2004). Recent studies on rock–bolt composite specimens have also examined dynamic cracking, energy dissipation and anchoring mechanisms under combined stress conditions (Wang et al. 2026). In contrast, the response of complete support systems remains less well understood. System behaviour

[*] Corresponding author. Email address: wangx@mail.neu.edu.cn

depends on the interaction between the shotcrete layer, mesh, plates, bolts and their connections, making it difficult to isolate the contribution of individual components.

In shotcrete–mesh–rockbolt systems, cracking of the shotcrete may significantly alter load-transfer mechanisms and affect the residual support capacity provided by the remaining mesh and reinforcement (Raffaldi et al. 2017; Stacey & Ortlepp 2001). Controlled dynamic testing is therefore needed to evaluate not only individual components but also their interaction at the system scale. Reviews of dynamic testing facilities have also shown that test configuration and boundary conditions influence the measured support response (Hadjigeorgiou & Potvin 2011; Xia et al. 2024).

Figure 1 shows 2 representative dynamic testing facilities used in previous studies. Large-scale impact facilities such as the Walenstadt testing facility have been used to study the dynamic behaviour of complete ground support systems and surface support configurations (Brändle et al. 2022; Brändle & Luis 2019; Vallejos et al. 2024). Laboratory-scale facilities have also been developed to investigate the response of load-distribution elements and their interaction with rockbolts and plates (Hinojosa et al. 2023). These studies have improved the understanding of support system behaviour, load-transfer and dynamic testing methodologies.



(a) (b)

Figure 1 Representative dynamic testing facilities used in previous studies. (a) Geobrugg Walenstadt test facility for large-scale ground support system testing; (b) Geobrugg Rancagua test facility for laboratory-scale load-distribution-element testing. Adapted from Brändle & Fonseca (2019) and Hinojosa et al. (2023)

Despite these advances, repeated-impact data for full-scale shotcrete–mesh–rockbolt panels remain limited. Most test programs focus on isolated components, single impacts or systems without a continuous shotcrete layer. Previous study also showed that mesh-test results depend strongly on test configuration and response metrics (Morkel et al. 2023). The effects of shotcrete cracking on residual deformation and rockbolt reactions under repeated impacts therefore remain insufficiently documented.

This work presents an indoor repeated dynamic drop testing program on a shotcrete–mesh–rockbolt ground support system using a newly developed FORTRESS (Full-scale Observation, Research, Testing on Resistance Evaluation for Support System)-Dyna apparatus. A C35 shotcrete panel reinforced with 8 mm welded mesh at

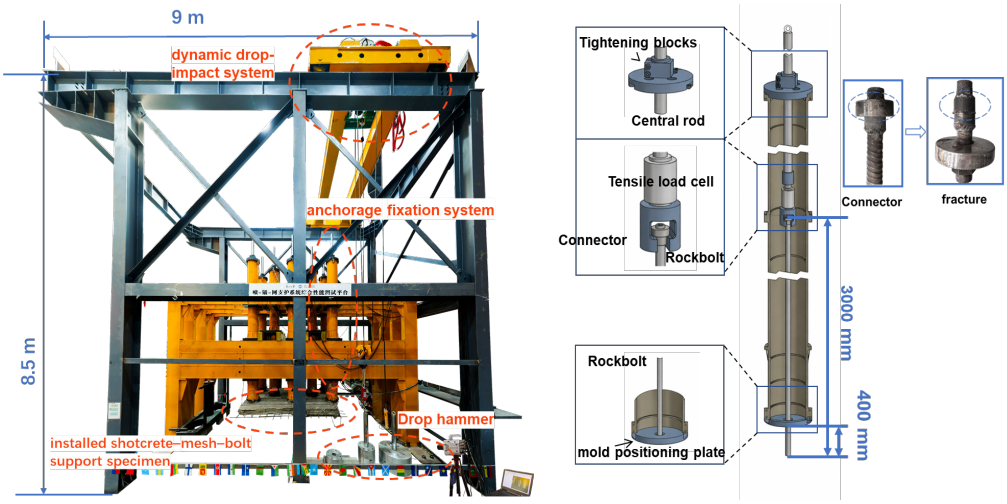
200 × 200 mm spacing and eight 3.0 m hollow threaded steel rockbolts was subjected to 24 repeated drop impacts. The study focuses on the global dynamic response, visible damage evolution and reactions of the central rockbolts. These results are used to summarise the observed stage-based response of the tested system. The interpretation is limited to the tested configuration, boundary condition and increasing impact sequence.

2 Dynamic laboratory tests

2.1 FORTRESS-Dyna apparatus and test configuration

The tests were conducted using the FORTRESS-Dyna apparatus: a newly developed full-scale indoor drop impact facility for ground support system testing. As shown in Figure 2a, FORTRESS-Dyna consists of a 9.0 m (l) × 8.5 m (h) rigid support frame with a remotely controlled overhead crane and modular drop weight assemblies. Different combinations of impact mass and release height can be applied, and the anchorage system allows full-scale support system specimens to be tested. In this study, a shotcrete–mesh–rockbolt support panel was suspended beneath the drop mass, and repeated out-of-plane impacts were applied to the central region of the panel in the vertical loading direction.

At the upper-end, each rockbolt was connected to a positioning rod through a test-specific connector and tensile load cell shown in Figure 2b. Connector fractures at B4 and B3 interrupted the corresponding upper reaction paths but did not involve the rockbolt bars. At the panel side, each rockbolt was fitted with a 200 × 200 × 8 mm plate.



(a) (b)

Figure 2 Test arrangement of the FORTRESS-Dyna apparatus. (a) Overall view of the test platform; (b) Rockbolt installation arrangement. The inset identifies the connector component that fractured at 2 central positions during the later impacts

A 512.0 kg drop mass was used in the first stage of testing and increased to 832 kg in the second stage. The nominal input energy for each impact is calculated as

$$E_{n,i} = m_i g h_i \tag{1}$$

where:

$E_{n,i}$ = nominal input energy of the ith impact

m_i = drop mass

g = gravitational acceleration

h_i = designed release height.

To approximately account for the additional gravitational work after impact, an estimated input energy was also calculated as

$$E_{H,i} = m_i g H_i = m_i g(h_i + \Delta u_i) \quad (2)$$

where:

- Δu_i = displacement of ground support system at final settled position after the impact
- H_i = corresponding total drop distance
- $E_{H,i}$ = estimated input energy (due to the post-contact motion is affected by shotcrete crushing, cracking and overall panel deformation).

Table 1 summarises the drop weight, release height and nominal input energy for each impact. It is worth pointing out that the cumulative nominal input energy is used only to describe the prescribed repeated-impact loading history and should not be interpreted as cumulative absorbed energy or as an equivalent single-impact energy. From Table 1, the cumulative nominal/estimated input energy are 64.4 and 66.8 kJ, respectively.

Table 1 Loading program in the tests

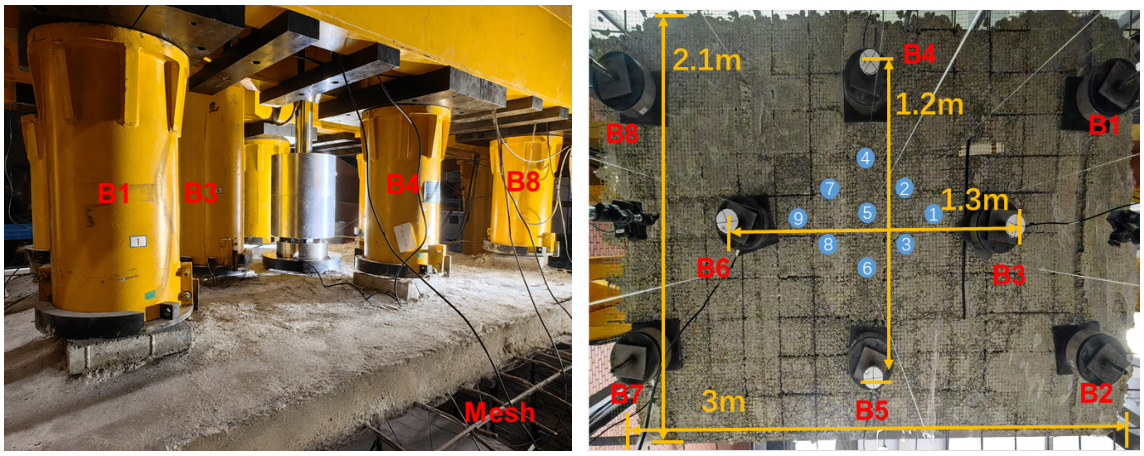
Case group	Impact label	Drop weight (kg)	Release height (cm)	Nominal input energy per impact (kJ)	Number of impacts	Cumulative nominal input energy at end of group (kJ)	Cumulative estimated input energy at end of group (kJ)
512-20	512-20-1 512-20-2 512-20-3	512	20	1.00	3	3.0	3.0
512-30	512-30-1 512-30-2 512-30-3		30	1.51	3	7.5	7.5
512-40	512-40-1 512-40-2 512-40-3		40	2.01	3	13.6	13.6
512-50	512-50-1 512-50-2 512-50-3		50	2.51	3	21.1	21.1
512-60	512-60-1 512-60-2 512-60-3		60	3.01	3	30.1	30.2
832-30	832-30-1	832	30	2.45	1	32.6	32.7
832-40	832-40-1 832-40-2 832-40-3		40	3.27	3	42.4	42.7
832-50	832-50-1 832-50-2 832-50-3		50	4.08	3	54.6	55.7
832-60	832-60-1 832-60-2		60	4.90	2	64.4	66.8

2.2 Shotcrete–mesh–rockbolt system

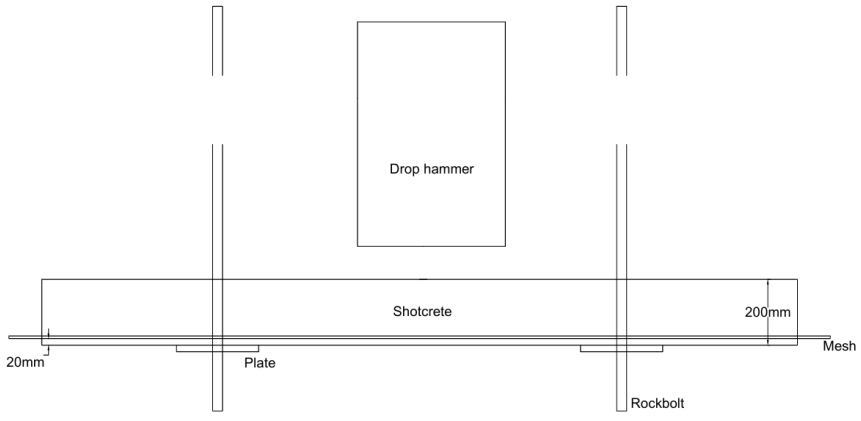
The tested support system consisted of a C35 shotcrete panel, welded steel mesh, 8 rockbolts, plates and end connection components. The concrete mix, sand, weld mesh and rockbolts were chosen and shipped from the field support materials that used in a real tunnelling project. The main specimen parameters are listed in Table 2, and Figure 3 shows the installed panel, rockbolt layout, and schematic cross-section.

The rockbolts were installed using the mechanical end-anchorage configuration shown in Figure 2b. The specimen was prepared on a steel base plate following the field installation sequence as closely as practicable: the 8 rockbolts were first positioned according to the designed layout, the welded mesh was then installed on the plate side and supported at the bearing plates, and the mixed C35 shotcrete material was finally placed on the mesh panel to form a 200 mm thick panel. The C35 layer covered the mesh and the rockbolt sections passing through the panel, producing bond between these components within the panel. The shotcrete panel was then cured for one month before the dynamic drop testing.

As shown in Figure 3c, the welded mesh is located approximately 20 mm from the plate-side surface, corresponding to approximately 180 mm from the impact-side surface. During testing, the drop weight impacts the upper central surface of the panel. Rockbolts B3, B4, B5, and B6 are located around the central impact region, while B1, B2, B7 and B8 are located near the panel boundaries.



(a) (b)



(c)

Figure 3 Shotcrete–mesh–rockbolt support system. (a) Installed support panel beneath the drop weight; (b) Rockbolt numbering and description of central and edge areas; (c) Schematic cross-section showing the impact-side surface, plate-side surface, panel thickness and mesh spatial location

Table 2 Specific parameters of the shotcrete–mesh–rockbolt system

Item	Value
C35 concrete	Approximately 35 MPa uniaxial compressive strength
Panel size	2,100 × 3,000 mm
Panel thickness	200 mm
Curing time	30 days
Mesh spacing	200 × 200 mm
Mesh steel tendon diameter	8 mm
Mesh position	20 mm from plate-side surface
Rockbolt length	3.0 m
Rockbolt outer/inner diameter	25 mm/15 mm
Rockbolt elastic modulus	206 GPa
Plate dimension	200 × 200 × 8 mm

2.3 Monitoring system

The monitoring system recorded impact force, panel displacement, rockbolt reactions and visible damage evolution. Figure 4 shows the monitoring layout used in the test.

The drop weight was instrumented with an accelerometer and an impact force sensor to record the impact input. String potentiometers were arranged beneath the support panel at the locations marked in Figure 3b. The centre transducer (Point 5 in Figure 3b) was used to determine the peak and residual displacement values discussed in Section 3.1.

Rockbolt reactions used in this study were recorded by upper-end tensile load cells incorporated into the rockbolt installation assemblies shown in Figure 2b. Auxiliary lower-end load cells were also installed under the plate to check the lower-side response during testing, but these records are not interpreted quantitatively in this work to keep the paper concise.

Visible cracking and damage states were documented using digital photographs acquired after each impact for qualitative interpretation. Table 3 summarises the measured parameters and corresponding instruments.



(a) (b)

Figure 4 Monitoring layout used in the impact test. (a) Accelerometer and impact force sensor installed on the drop weight; (b) Lower-end load cells, string potentiometers

All dynamic sensors were connected to a DH5922D 64-channel data acquisition system. The sampling frequency was 10 kHz during the impact sequence. In this work, the main analysis uses the impact force, centre displacement, upper-end rockbolt reactions and visual damage records.

Table 3 Measuring layout used in the impact test

Monitoring object	Instrumentation	Main output
Drop weight	Accelerometer and impact force sensor	Impact input, peak impact force and contact duration
Support panel	String potentiometers	Residual displacement
Rockbolt	Upper-end and lower-end load cells	Rockbolt end reactions
Damage process	Post-impact photographs	Visible crack development and damage state

3 Test results and discussion

The results are presented in terms of global visible damage evolution, dynamic response and reactions of the central rockbolts. These observations are used to describe the progressive degradation of the tested support system under repeated impacts.

3.1 Damage evolution of the shotcrete–mesh–rockbolt support

Figure 5 shows the selected typical photos of the visible damage evolution during the repeated-impact tests. The damage developed progressively with increasing number of impacts and cumulative nominal input energy.

During the early impacts, the shotcrete panel remained largely intact, with only minor surface disturbance near the impact region. A clear visible crack first appeared during the later impacts of the 512 kg sequence. With continued impacts, the crack extended and became increasingly continuous. At 512-60-2, a continuous crack propagated to the panel edge and through the full 200 mm panel thickness, hereafter referred to as through-going visible major cracking.



(a) (b) (c) (d)

Figure 5 Representative damage evolution of the tested shotcrete–mesh–rockbolt support system showing (a) initial visible cracking at 512-30-3, (b) through-going visible major cracking at 512-60-2, (c) pronounced crack opening and local block movement at 832-50-2, and (d) final instability at 832-60-2

Following the transition to the 832 kg sequence, damage was characterised primarily by crack openings and relative movement between cracked shotcrete blocks. During the final impacts, large deformation, local fragmentation and exposure of the welded mesh were observed, indicating that the shotcrete layer had largely lost its continuous plate-like action.

3.2 Global dynamic response of repeated dynamic impacts

The global response of the support system was evaluated using the impact force recorded by the force sensor mounted on the drop hammer and the centre displacement measured at Point 5 (Figure 3b). The main indicators include peak impact force, contact duration, downward residual displacement, and normalised apparent impact stiffness. To provide direct context for these extracted quantities, Figure 6 presents representative measured time histories from a relatively high-level impact (832-50-1 case).

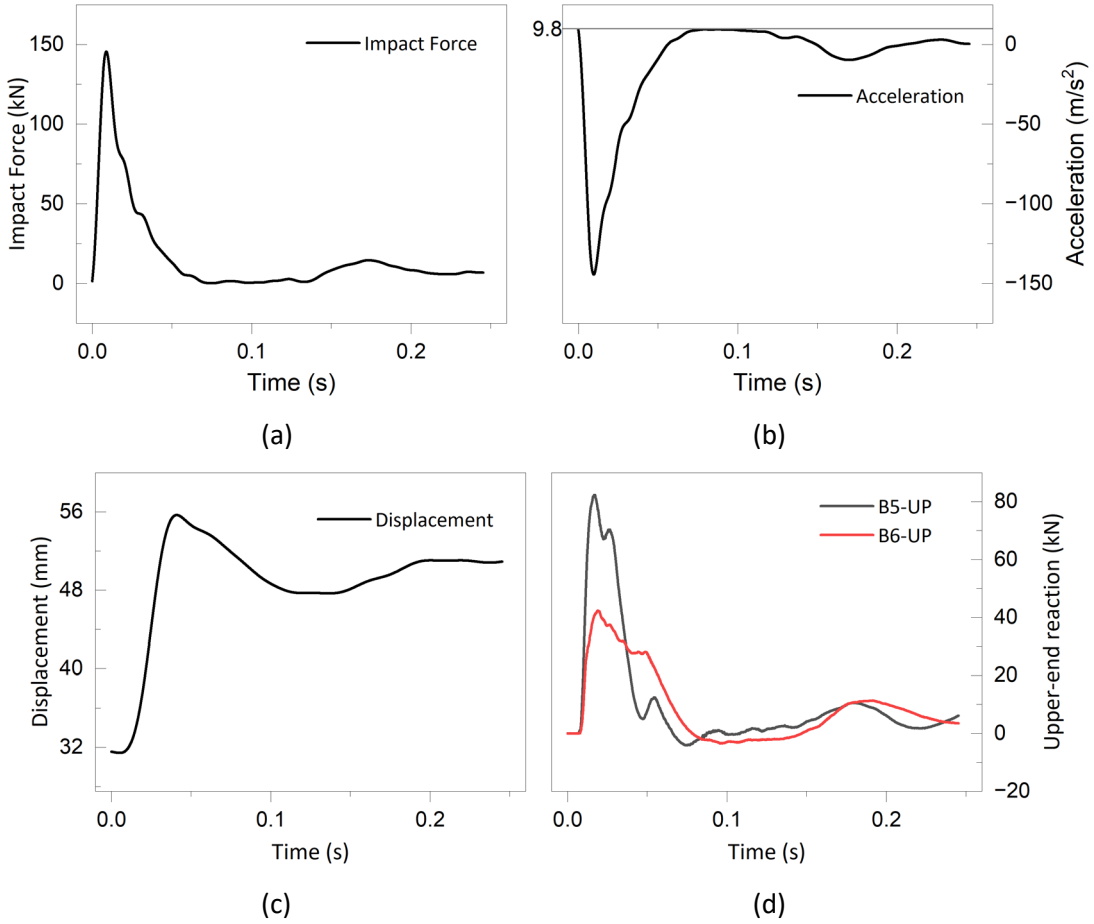


Figure 6 Representative measured time histories for impact 832-50-1. (a) Impact force; (b) Acceleration; (c) Central displacement; (d) B5 and B6 upper-end reactions

The impact force exhibited a pronounced initial peak followed by a lower-amplitude secondary response. The acceleration record showed a corresponding transient response during the initial impact, while the central displacement increased rapidly to its peak before partial recovery. Measurable upper-end reactions were recorded at both B5 and B6 during the same event.

Figure 7 shows that the peak impact force fluctuated during the test and did not increase monotonically with nominal input energy. A maximum value of approximately 182.69 kN was recorded during impact 512-60-1. After the transition to the 832 kg impact series, the nominal input energy per impact increased, but the peak impact force did not increase correspondingly, with several later impacts producing lower peak forces. In contrast, the contact duration gradually increased during the later stages of testing and reached approximately 0.154 s in the final impact. This increase in contact duration indicates a progressive reduction

in system stiffness as panel damage accumulated. The deformation response is examined further using the centre residual displacement in Figure 8.

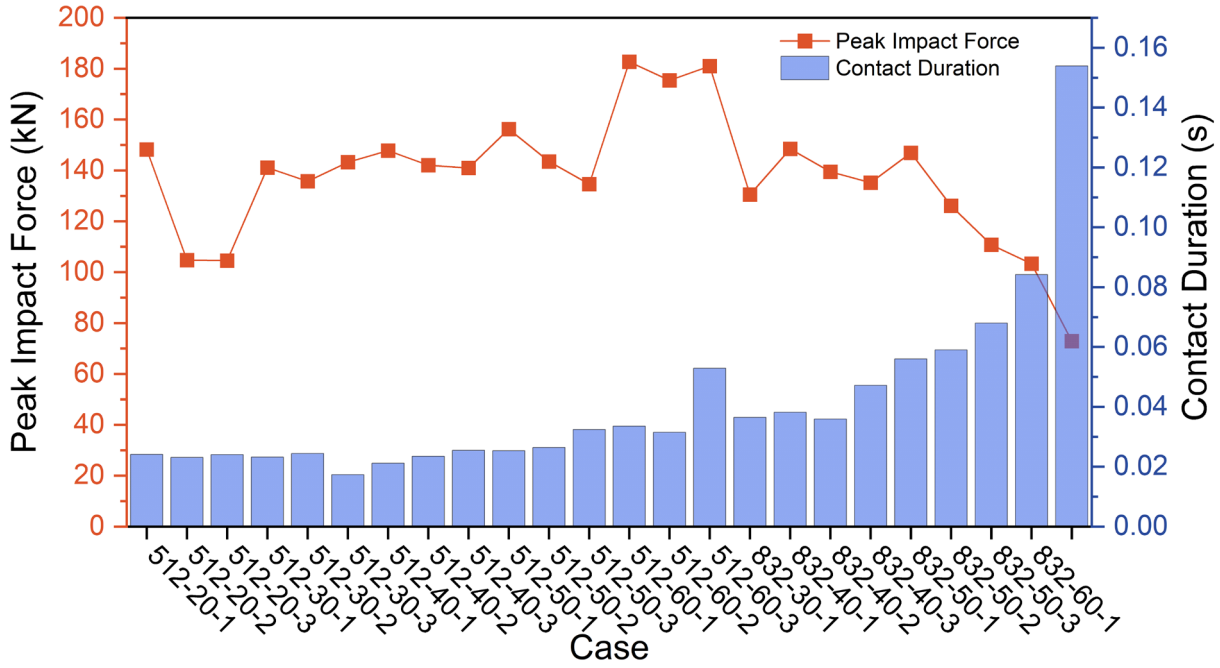


Figure 7 Evolution of peak impact force and contact duration during repeated impacts

Downward residual displacement is calculated from the centre displacement record on an impact-by-impact basis as:

$$u_{r,i} = u_{0,i+1} - u_{0,1} \tag{3}$$

where:

$u_{0,1}$ = centre displacement before the first impact

$u_{0,i+1}$ = settled centre displacement recorded before the subsequent impact.

For the final impact, $u_{0,i+1}$ was replaced by the final stable displacement recorded after the system had stabilised. Positive value represents downward residual movement of the support panel.

Figure 8 shows the evolution of downward residual displacement with cumulative nominal input energy. Residual displacement remained limited before through-going visible major cracking and increased only gradually with increasing energy input. At 512-60-2, where a through-going visible major crack was first observed, the cumulative nominal input energy is 27 kJ and the residual displacement is approximately 7.3 mm. Following through-going visible major cracking, residual displacement accumulated much more rapidly, particularly during the 832 kg impact sequence. The residual displacement reached approximately 45.6 mm at 832-40-3 and 307 mm in the final impact. This rapid increase in residual displacement shows that through-going visible major crack marked the transition to a deformation-dominated response of the damaged panel.

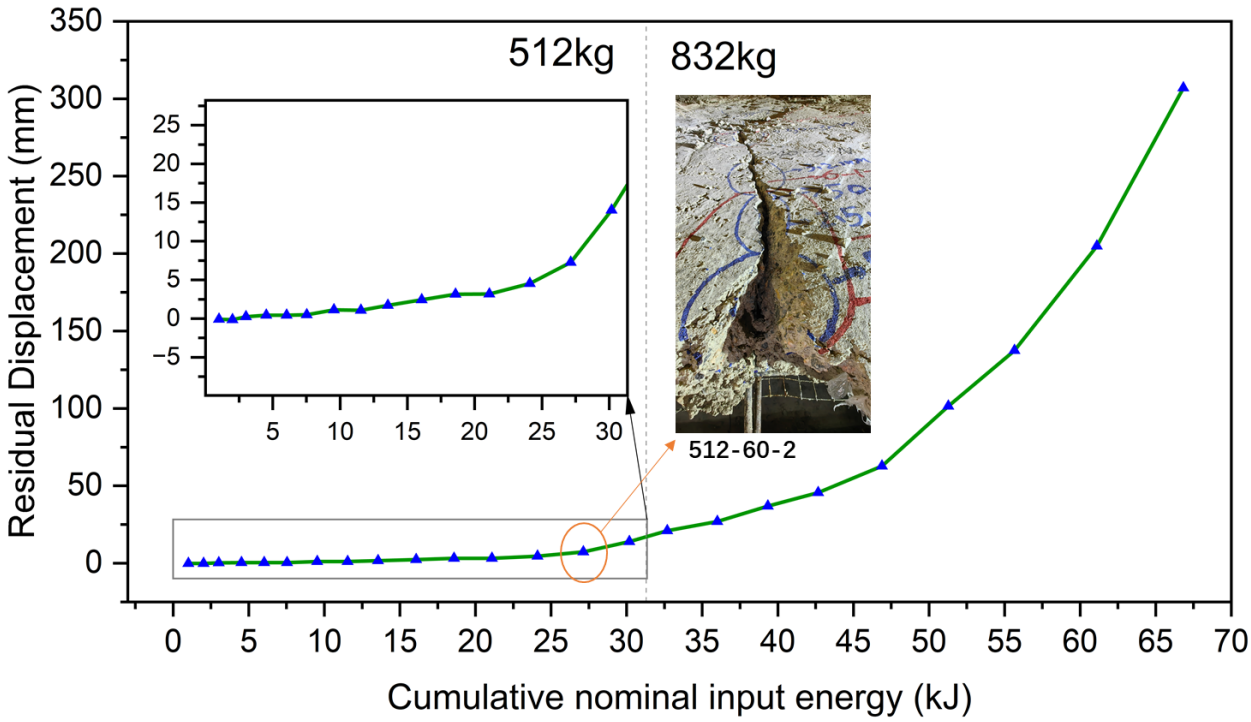


Figure 8 Evolution of downward residual displacement with cumulative nominal input energy. The zoom-in insert shows the early-stage response before rapid displacement accumulation

Apparent impact stiffness for each impact is calculated as:

$$K_i = \frac{F_{p,i}}{u_{p,i}} \tag{4}$$

where:

Ki = the apparent impact stiffness of the ith impact

$F_{p,I}$ = the peak impact force

$u_{p,I}$ = the corresponding peak displacement measured at the panel centre.

The apparent impact stiffness is used only as a relative indicator of stiffness degradation under the present loading path. Because the first impact is affected by initial seating, the reference stiffness is defined as:

$$K_{ref} = \frac{K_2+K_3}{2} \tag{5}$$

where:

K_{ref} = the reference stiffness, defined as the mean apparent impact stiffness of the second and third impacts, denoted by K_2 and K_3, respectively.

The normalised apparent impact stiffness is then calculated as:

$$\overline{K_i} = \frac{K_i}{K_{ref}} \tag{6}$$

where:

$\overline{K_i}$ = the dimensionless normalised apparent impact stiffness of the ith impact.

Figure 9 shows the reduction of normalised apparent impact stiffness with cumulative nominal input energy. The first data point is shown for completeness, but mainly reflects initial seating of the test system. During the early impacts, the normalised stiffness remained close to the reference level, with values of approximately 0.95–1.05. As cracking and residual displacement accumulated, the stiffness decreased

progressively. It decreased to 0.37 at a cumulative nominal input energy of 30 kJ and subsequently to 0.16 during the 832 kg impact sequence. In the final impacts, the normalised stiffness approached 0.01, corresponding to a reduction of more than 98% relative to $\overline{K}$. This reduction indicates that the panel had largely lost its initial resistance to out-of-plane impact deformation.

Overall, the global response was characterised by progressive stiffness degradation and increasing residual deformation under repeated impacts. Residual displacement, contact duration and apparent impact stiffness provided consistent indicators of this degradation.

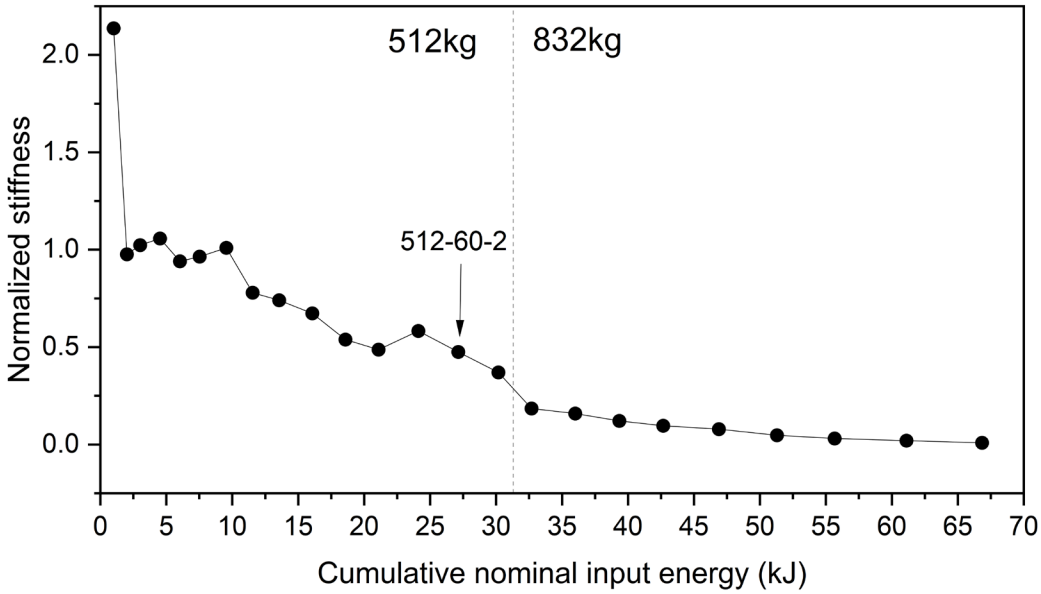


Figure 9 Evolution of normalised apparent impact stiffness with cumulative nominal input energy

3.3 Reactions of central rockbolts

The 4 central rockbolts, B3–B6, were closet to the impact region, and their peak upper-end reactions are shown in Figure 10. Before through-going visible major cracking, all 4 rockbolts developed measurable reactions. The reactions of the 4 rockbolts were non-uniform, as some rockbolts subject approximately 80–90 kN and other rockbolts only suffer around 30–50 kN. This difference is consistent with the uneven cracking and deformation of the panel. To sum, all the rockbolts do not reach to the yielding load level and the rockbolts are acted as elastic restraints during this repeated dynamic impact test.

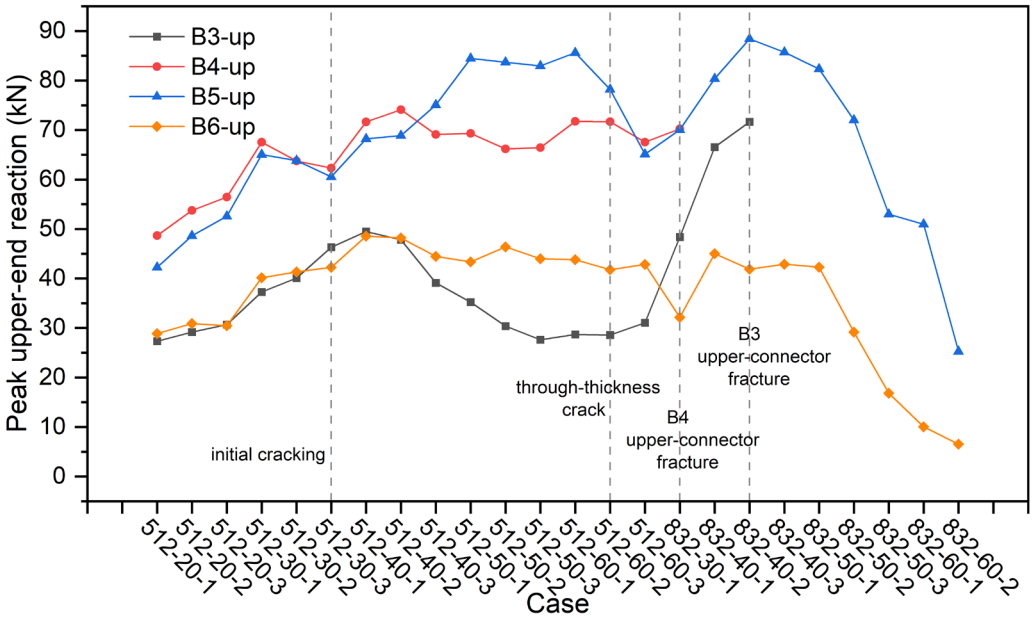


Figure 10 Peak reactions of the central rockbolts B3–B6 during repeated impacts

B4 reached 70.2 kN at 832-30-1, when its upper connector fractured, and its upper-end reaction was treated as unavailable thereafter. B3 reached 71.6 kN at 832-40-2 before the corresponding upper connector fractured and was treated in the same manner. In contrast, B5 and B6 continued to record measurable reactions during impacts 832-40-1 to 832-40-3, ranging from approximately 80.4–88.4 kN and 41.9–45.0 kN, respectively.

During the later impacts, the B5 and B6 reactions decreased to approximately 25.3 and 6.5 kN at 832-60-2. Thus, loss of the B3 and B4 upper connections did not immediately eliminate restraint at the other central positions, although their reactions weakened as panel damage progressed.

4 Conclusions

A full-scale shotcrete–mesh–rockbolt support panel was subjected to 24 repeated drop impacts using the newly developed FORTRESS-Dyna apparatus. The program examined progressive damage under repeated loading rather than the full deformation capacity of the rockbolts. The main conclusions are:

- Visible damage developed from local sparse cracking to through-going visible major cracking, crack opening, block movement and final instability of the test panel. The observed crack opening and block movement explain the rapid deformation accumulation during the later impacts.
- Peak impact force alone did not capture the progressive degradation of the tested support system. Contact duration, downward residual displacement and normalised apparent impact stiffness provided more useful indicators of damage accumulation under repeated impacts.
- Using cumulative nominal input energy as the loading progression index, a clear change in deformation response was observed after the formation of through-going visible major cracking. The residual displacement was 7.3 mm when the through-crack formed at a cumulative nominal input energy of 27 kJ, but increased rapidly under subsequent impacts and reached approximately 307 mm in the final impact. This response was accompanied by continued degradation of the apparent impact stiffness, indicating a large reduction in the post-cracking resistance of the tested support system.
- After through-going visible major cracking, the support response of shotcrete-mesh-bolt system became increasingly dependent on the remaining rockbolt–plate–mesh load-transfer paths. Within the tested impact range, damage was concentrated mainly in the shotcrete–mesh layer and the

connection components, while the rockbolts remained largely elastic. The fracture of the B4 and B3 upper connectors did not immediately result in system instability because B5 and B6 continued to provide residual restraint during subsequent impacts. These observations suggest that alternative load-transfer paths can maintain limited support capacity after shotcrete cracking, although the capacity degraded progressively under continued impact loading.

- Future work will relate the measured support response to seismic demand in underground mines, considering event magnitude, ground motion and rock ejection.

Acknowledgement

The authors gratefully acknowledge financial support from the National Natural Science Foundation of China (Grant Nos. 52374083) and the Science and Technology Program of Liaoning Province (Grant Nos. 2025JH2/101330167, No. 2023JH1/10400004). The authors also want to thank the members of the Geomechanics Research Group for their assistance in the specimen preparation, instrumentation and the dynamic impact tests.

References

Brändle, R, Luis Fonseca, R, von Rickenbach, G, Fischer, G, Vallejos, JA, Marambio, E … Cuello, D 2022, 'Large-scale dynamic testing of ground support systems at the Walenstadt testing facility', in Y Potvin (ed.), *Caving 2022: Proceedings of the Fifth International Conference on Block and Sublevel Caving*, Australian Centre for Geomechanics, Perth, pp. 177–190, https://doi.org/10.36487/ACG_repo/2205_10

Brandle, R & Luis Fonseca, R 2019, 'Dynamic testing of surface support systems', in J Hadjigeorgiou & M Hudyma (eds), *Ground Support 2019: Proceedings of the Ninth International Symposium on Ground Support in Mining and Underground Construction*, Australian Centre for Geomechanics, Perth, pp. 243–250, https://doi.org/10.36487/ACG_rep/1925_15_Brandle

Cai, M 2024, 'Rockburst risk control and mitigation in deep mining', *Deep Resources Engineering*, vol. 1, no. 2.

Cai, M & Kaiser, PK 2018, *Rockburst Support Reference*, MIRARCO, Sudbury.

Chunlin Li, C 2010, 'A new energy-absorbing bolt for rock support in high stress rock masses', *International Journal of Rock Mechanics and Mining Sciences*, vol. 47, no. 3, pp. 396–404.

Hadjigeorgiou, J & Potvin, Y 2011, 'A critical assessment of dynamic rock reinforcement and support testing facilities', *Rock Mechanics and Rock Engineering*, vol. 44, no. 5, pp. 565–578.

He, B-G, Li, H-P, Feng, X-T, Zhu, Z-H, Liu, H-Y, Zhang, H-Y, & Meng, X-R 2025, 'Generation of and countermeasures against time-delayed rockbursts', *Deep Resources Engineering*, vol. 2, no. 3.

Hinojosa, M, Vallejos, JA, Marambio, E, Suzuki, K, Fischer, G & von Rickenbach, G 2023, 'A laboratory-scale dynamic test of load distribution elements at Rancagua testing facility', in J Wesseloo (ed.), *Ground Support 2023: Proceedings of the 10th International Conference on Ground Support in Mining*, Australian Centre for Geomechanics, Perth, pp. 411–424, https://doi.org/10.36487/ACG_repo/2325_27

Kaiser, PK & Moss, A 2022, 'Deformation-based support design for highly stressed ground with a focus on rockburst damage mitigation', *Journal of Rock Mechanics and Geotechnical Engineering*, vol. 14, no. 1, pp. 50–66.

Knox, G 2023, 'Laboratory-based drop testing of rock reinforcement', in J Wesseloo (ed.), *Ground Support 2023: Proceedings of the 10th International Conference on Ground Support in Mining*, Australian Centre for Geomechanics, Perth, pp. 23–38, https://doi.org/10.36487/ACG_repo/2325_0.02

Li, CC 2021, 'Principles and methods of rock support for rockburst control', *Journal of Rock Mechanics and Geotechnical Engineering*, vol. 13, no. 1, pp. 46–59.

Morkel, IG, Mikula, PA & Whiting, RK 2023, 'A review of ground support mesh testing around the world', in J Wesseloo (ed.), *Ground Support 2023: Proceedings of the 10th International Conference on Ground Support in Mining*, Australian Centre for Geomechanics, Perth, pp. 373–398, https://doi.org/10.36487/ACG_repo/2325_25

Raffaldi, MJ, Martin, LA, Benton, DJ, Sunderman, CB, Stepan, MA & Powers, MJ 2017, 'Quasi-static and mechanical shock testing of reinforced shotcrete surface support', in J Wesseloo (ed.), *Deep Mining 2017: Proceedings of the Eighth International Conference on Deep and High Stress Mining*, Australian Centre for Geomechanics, Perth, pp. 733–746, https://doi.org/10.36487/ACG_rep/1704_50_Raffaldi

Shou, Y, Guo, L, & Zhou, X 2024, 'Development of the rolling extrusion rock bolt with constant resistance and large deformation', *Deep Resources Engineering*, vol. 1, no. 1.

Stacey, R & Ortlepp, WD 2001, 'Tunnel surface support - Capacities of various types of wire mesh and shotcrete under dynamic loading', *Journal of the South African Institute of Mining and Metallurgy*, vol. 101, pp. 337–342.

Vallejos, JA, Marambio, E, Burgos, L, Cuello, D, Brändle, R, Luis, R, Von Rickenbach, G, & Fischer, G 2024, 'Dynamic test response of ground support systems for underground excavations at the Walenstadt testing facility', *Rock Mechanics and Rock Engineering*, vol. 57, no. 1, pp. 389–428.

Villaescusa, E & Potvin, Y (eds) 2004,'Dynamic testing of rock reinforcement using the momentum transfer concept', *Ground Support in Mining and Underground Construction*, CRC Press, Boca Raton, pp. 614–642.

Wang, L, Huang, T, Ren, F, Chang, Y, & Xu, Z 2026, 'Dynamic responses of coal-rock-bolt composite with axial pre-stress and confining pressure', *Deep Resources Engineering*, vol. 3, no. 2.

Xia, K, Wang, M, Fu, Y, Wu, B, Xu, Y, & Yao, W 2024, 'Advances in dynamic test of deep rocks considering in-situ mechanical and hydraulic conditions', *Deep Resources Engineering*, vol. 1, no. 2.